AN ESTIMATE OF THE TRIPLE POINT NUMBERS OF SURFACE-KNOTS BY QUANDLE COCYCLE INVARIANTS

ERI HATAKENAKA

Abstract. The triple point number of a surface-knot is defined to be the minimal number of triple points among all diagrams of the surface-knot. We give a lower bound of the triple point number using quandle cocycle invariants.

1. Introduction

A *surface-knot* is, by definition, a connected or disconnected closed surface embedded into $\mathbb{R}^4$ locally flatly. Two surface-knots are said to be *equivalent* if they are related by an ambient isotopy of $\mathbb{R}^4$. Let $\pi : \mathbb{R}^4 \to \mathbb{R}^3$ be a projection, and let $F \subset \mathbb{R}^4$ be a surface-knot. We can assume that the singular set of $\pi(F)$ consists of double points, isolated triple points, and isolated branch points (shown in Figure 1) by perturbing $F \subset \mathbb{R}^4$ if necessary. A *surface-knot diagram* of F will be $\pi(F)$ with information near the crossing part with respect to the projection. The *triple point number* of F is defined to be the minimal number of triple points among all diagrams of a surface-knot equivalent to F. We denote it by $t(F)$.

A *2-knot* is a surface-knot by a 2-sphere. There are two well-known families of surface-knots; ribbon 2-knots and twist spun of classical knots. It is known in [12] that a 2-knot F is a ribbon 2-knot if and only if $t(F) = 0$. Satoh [6] showed that there is no surface-knot F with $t(F) = 1$. Moreover, it is known in [8] and [9] that there is no 2-knot F with $1 \leq t(F) \leq 3$. In [10], Satoh and Shima gave a lower bound of the triple point numbers using quandle cocycle invariants associated with the dihedral quandle R_3 of order three. Using this theorem, they showed that the triple point number of the 2-twist-spun trefoil is four.

In this paper, we refine their lower bound by using another quandle, the dihedral quandle R_5 of order five. The main theorem of this paper is

Theorem 1.1. *Let θ be a 3-cocycle of the dihedral quandle R_5 with a coefficient group G. If the quandle cocycle invariant $\Phi_\theta(F) \in \mathbb{Z}[G]$ of an oriented surface-knot F satisfies that $\Phi_\theta(F) \notin \mathbb{Z} \subset \mathbb{Z}[G]$, then $t(F) \geq 6$.*

Using this theorem, we can show the fact that the triple point numbers of the 2-twist-spun figure eight knot and the 2-twist-spun (2,5) torus-knot are at least six, which could not be obtained by using the theorem in [10].

This paper is organized as follows. In Section 2, we review surface-knots and quandle cocycle invariants for surface-knots. Section 3 is devoted to prove Theorem 1.1. In section 4, we give some lemmas and review Alexander numberings, for the proof of Theorem 1.1. In section 5, we give two examples which we can obtain by Theorem 1.1.

2000 *Mathematics Subject Classification.* Primary 57Q45; Secondary 57Q35.

Acknowledgment. The author would like to thank Tomotada Ohtsuki for encouraging her. She is grateful for valuable suggestions to J. Scott Carter, Seiichi Kamada, Akiko Shima, and Shin Satoh. She would like to thank Sadayoshi Kojima for his helpful comments on the draft, and Hiroshi Ooyama for his support on computer programs.

2. Preliminaries

In Section 2.1 we review surface-knots and surface-knot diagrams. In Section 2.2 we review quandle cocycle invariants for surface-knots.

2.1. **Surface-knots.** Let Σ be a closed surface, and let $f : \Sigma \to \mathbb{R}^4$ be a locally flat embedding of Σ into $\mathbb{R}^4$. The image $f(\Sigma)$ is called a *surface-knot*. A surface-knot $F(= f(\Sigma))$ is called *oriented* if Σ is oriented. Let $\pi : \mathbb{R}^4 \to \mathbb{R}^3$ be a projection of $\mathbb{R}^4$ onto $\mathbb{R}^3$. The closure of the self-intersection set of $\pi(F)$ is called the *singular set*. For a point $x \in \pi(F)$, if $\#(\pi^{-1}(x) \cap F) = 2$ (or 3, respectively) then x is called a *double point* (or *triple point*). See the left hand side of Figure 1 (A) (or (B)). If $x \in \pi(F)$ is a point such that for any small neighborhood $N(x)$, the intersection of $N(x)$ and $\pi(F)$ contains a cone on a figure 8, then x is called a *branch point*. See the left hand side of Figure 1 (C). A projection π is called *generic* for F if the singular set of $\pi(F)$ consists of double points, isolated triple points, and isolated branch points. By perturbing F if necessary, we may assume that π is generic.

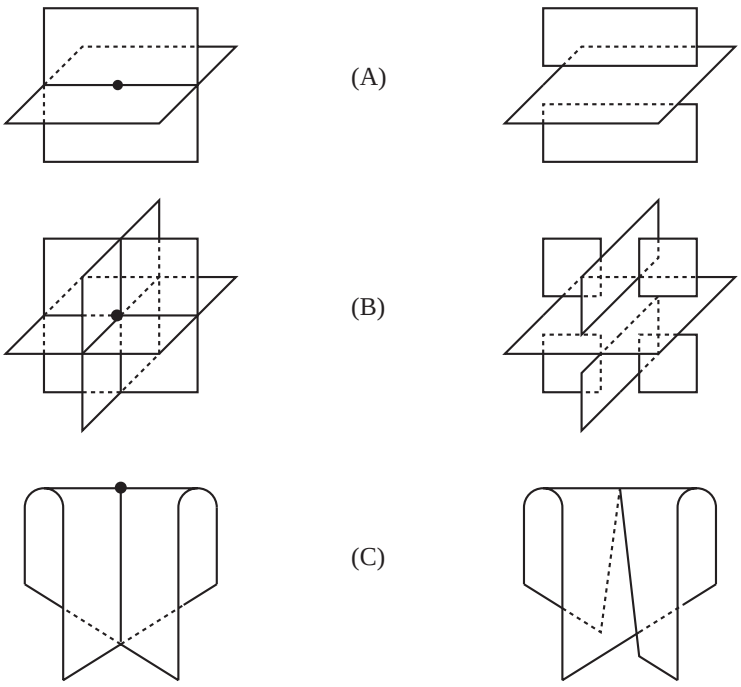

Figure 1. Projection images (left) and diagrams (right) in neighborhoods of a double point (A), a triple point (B), and a branch point (C)

Along each double point curve, two sheets are intersecting, and one of the sheets (called the *over-sheet*) is higher than the other (called the *under-sheet*) with respect to the projection. In a small neighborhood of a triple point, there are three sheets which we call the *top,* the *middle,* and the *bottom sheets* with respect to the projection. To distinguish higher and lower sheets, the under-sheet will be depicted by breaking along the double point curve. A *surface-knot diagram* is a generic projection image $\pi(F)$ with such additional crossing information. See the right hand side of Figure 1.

2.2. **Quandle cocycle invariants for surface-knots.** A *quandle* is defined to be a set X with a binary operation $* : X \times X \to X$ satisfying the following properties:

(Q1) For each $x \in X$, $x * x = x$.
(Q2) For any $x, y \in X$, there is a unique element $z \in X$ such that $x = z * y$.
(Q3) For any $x, y, z \in X$, $(x * y) * z = (x * z) * (y * z)$.

For any group G, the *conjugation quandle* of G is defined to be the group G with the binary operation $x * y = y^{-1}xy$. Any conjugacy class of G is a subquandle of the conjugation quandle of G.

The *dihedral quandle* R_n of order n is defined by the set $\{0, 1, ..., n-1\}$ with the operation $x * y = 2y - x \pmod n$, which is a subquandle of the conjugation quandle of the dihedral group of order $2n$, consisting of reflections.

For a quandle and an abelian group, we can define the homology and the cohomology groups ([2]). We review 3-cocycles here. Let X be a finite quandle, and G an abelian group written multiplicatively. A map $\theta : X \times X \times X \to G$ is called a 3-*cocycle* of X with the coefficient group G if it satisfies the following conditions:

(i) For any $x, y \in X$, $\theta(x, x, y) = \theta(x, y, y) = 1_G$.
(ii) For any $x, y, z, w \in X$,

$$\theta(x, z, w) \cdot \theta(x * z, y * z, w) \cdot \theta(x, y, z) = \theta(x * y, z, w) \cdot \theta(x, y, w) \cdot \theta(x * w, y * w, z * w).$$

As an example of 3-cocycles, in [4] (or [5]), Mochizuki gave an explicit presentation of a 3-cocycle $\theta : R_5 \times R_5 \times R_5 \to \mathbb{Z}_5 = \langle u | u^5 = 1 \rangle$ defined by

$$(\sharp) \qquad \theta(x, y, z) = u^{(y-x)(3z^5+2y^3z^2+2y^2z^3+3yz^4+3xy^3z+xy^2z^2+2xyz^3+4xz^4)}.$$

It will be used to calculate the quandle cocycle invariants concretely in Section 5.

We define a color of a surface-knot diagram. Throughout this paper, we assume that surface-knots are oriented. Given a surface-knot F, we take a normal vector $\vec{n}$ to the projection $\pi(F)$ in $\mathbb{R}^3$ such that the triplet $(\vec{v_1}, \vec{v_2}, \vec{n})$ matches the orientation of $\mathbb{R}^3$, where $(\vec{v_1}, \vec{v_2})$ gives the orientation of F. Let X be a finite quandle, and D a diagram of F. Recall that a surface-knot diagram is represented by a disjoint union of compact surfaces, which are called *broken sheets.* For a diagram D, let $\mathcal{B}(D)$ be the set of its broken sheets. Along a double point curve, there exist three broken sheets locally, some of which may coincide. Let $H_1, H_1', H_2 \in \mathcal{B}(D)$ be such sheets such that H_1, H_1' are the under-sheets, and H_2 is the over-sheet. Assume that the normal vector to H_2 points to H_1'. See the left hand side of Figure 2. A *color* on D in X is a map $C : \mathcal{B}(D) \to X$ satisfying $C(H_1) * C(H_2) = C(H_1')$. D is said to be *colored* by X if D has a color in X. Note that the number of colors on D is independent of a choice of diagrams.

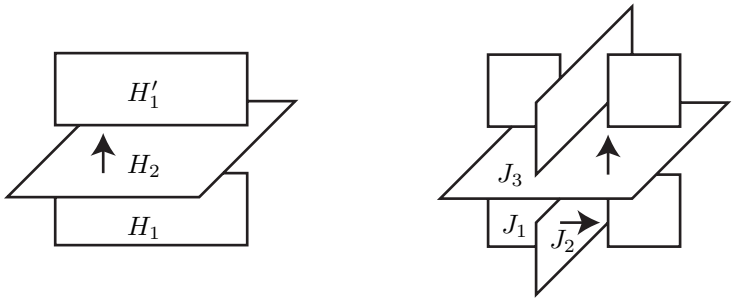

FIGURE 2. Three broken sheets along a double point curve (left), and seven broken sheets around a triple point (right)

A color of a triple point is given as follows. Around a triple point of a diagram, there exist seven broken sheets locally, some of which may coincide. Let $J_1, J_2, J_3 \in \mathcal{B}(D)$ be the broken sheets such that J_1 is the bottom sheet from which the normal vectors to the middle and the top sheets point outwards, J_2 is the middle sheet from which the normal vector to the top sheet points outwards, and J_3 is the top sheet. See the right hand side of Figure 2. The *color* of a triple point of D colored by X is the triplet $(C(J_1), C(J_2), C(J_3)) \in X \times X \times X$.

Let n_1, n_2, and n_3 be the normal vectors to the bottom, the middle, and the top sheets around a triple point τ, respectively. The *sign* of τ is 1 if the triplet (n_1, n_2, n_3) matches the orientation of $\mathbb{R}^3$, and -1 otherwise. We denote the sign of τ by $\epsilon(\tau) \in \{\pm 1\}$.

For a fixed 3-cocycle $\theta : X \times X \times X \to G$ and a color C on D in X, we define the *weight* at τ by

$$W_\theta(\tau; C) = \theta(x, y, z)^{\epsilon(\tau)} \in G,$$

where $(x, y, z) \in X \times X \times X$ is the color of τ. Further we put

$$W_\theta(C) = \prod_\tau W_\theta(\tau; C) \in G,$$

where the product is taken over all triple points of D. The *quandle cocycle invariant* of F associated with θ is defined by

$$\Phi_\theta(F) = \sum_C W_\theta(C) \in \mathbb{Z}[G],$$

where the sum is taken over all possible colors on D. It is shown in [2] that $\Phi_\theta(F)$ is independent of a choice of diagrams of F by the 3-cocycle condition of θ. The augmentation of $\Phi_\theta(F)$ is equal to the number of colors on D, and so it is an invariant of F. $\Phi_\theta(F)$ can be regarded as a refinement of this invariant.

3. Proof of Theorem 1.1

The aim of this section is to prove Theorem 1.1. We give a proof in Section 3.5. In the proof, we will show that, if a surface-knot diagram has at most 5 triple points, then $W_\theta(C) = 1$ for any color C in R_5. To show this, we define colors on the singular set of a diagram in Section 3.1, and we classify types of colored triple

points in Section 3.2. Further, we list up admissible 4- and 5-tuples of types of colors of triple points in Sections 3.3 and 3.4 respectively.

3.1. **Colored singular set.** We regard the singular set of a surface-knot diagram as a disjoint union of

(i) a graph, which has 1- and 6-valent vertices corresponding to branch points and triple points respectively, and
(ii) circles, which has no vertices.

The graph and circles in a singular set may be linked in $\mathbb{R}^3$. An *edge* of a singular set will be an edge of this graph or a circle. Let τ be a triple point. There are six edges coming to τ. Such an edge is called a *b/m-, b/t-,* or *m/t-edge* if it is the intersection of bottom and middle, bottom and top, or middle and top sheets at τ respectively.

We define a color of an edge in R_5 as follows. Let D be a surface-knot diagram of an oriented surface-knot. Assume that D has a color $C : \mathcal{B}(D) \to R_5$, where $\mathcal{B}(D)$ is the set of broken sheets of D. If there are three broken sheets in the neighborhood of an edge as depicted in the left hand side of Figure 2, then the *color* of the edge is defined to be the pair $(C(H_1), C(H_2)) \in R_5 \times R_5$. A colored edge is called *degenerate* if $C(H_1) = C(H_2)$, and *nondegenerate* otherwise. The degeneracy condition does not depend on the orientation of the surface-knot.

Colors of edges around a triple point are given as follows. Let τ be a triple point of D. Recall that when D has a color, τ also has a color. If τ has a color $(a, b, c) \in R_5 \times R_5 \times R_5$, then there are two b/m-edges which have colors (a, b) and $(a * c, b * c)$, two b/t-edges which have colors (a, c) and $(a * b, c)$, and two m/t-edges which have the same color (b, c). See Figure 3.

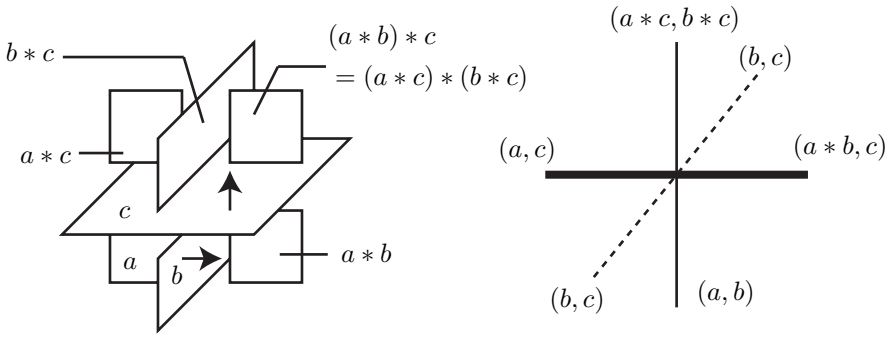

FIGURE 3. Colors of broken sheets (left) and edges (right) in a neighborhood of a triple point. In the right hand side, the b/m-, b/t-, and m/t-edges are depicted as thin lines, thick lines, and dotted lines respectively.

3.2. **Types of colors of a triple point.** We classify types of colored triple points. When a color of a triple point τ is a triplet $(a, b, c) \in R_5 \times R_5 \times R_5$, the triplet satisfies one of the following alternative conditions:

(1) $a = b = c$.
(2) $a = b \neq c$.

(3) $a \neq b = c$.
(4) $a = c \neq b$.
(5) a, b, c are distinct each other, and $c = a * b$.
(6) a, b, c are distinct each other, and $c \neq a * b$.

τ is said to be *of type* (n) for $n = 1, ..., 6$ if the triplet satisfies the condition (n). A triple point of type (1)−(3) is called *degenerate* and of type (4)−(6) *nondegenerate.* These types of τ and colors of edges around τ are listed in Table 1. In this table, $d(\tau)$ denotes the number of degenerate edges around τ. If we reverse the orientation of a surface-knot, then the types of colors change such as (1)↔(1), (2)↔(2), (3)↔(3), (4)↔(5), and (6)↔(6), but the degeneracy condition dose not change.

type of τ	color of τ	edges at τ			$d(\tau)$
		b/m-edges	b/t-edges	m/t-edges	
(1)	(a, a, a)	$(a, a), (a, a)$	$(a, a), (a, a)$	$(a, a), (a, a)$	6
(2)	(a, a, b)	$(a, a), (a * b, a * b)$	$(a, b), (a, b)$	$(a, b), (a, b)$	2
(3)	(a, b, b)	$(a, b), (a * b, b)$	$(a, b), (a * b, b)$	$(b, b), (b, b)$	2
(4)	(a, b, a)	$(a, b), (a, b * a)$	$(a, a), (a * b, a)$	$(b, a), (b, a)$	1
(5)	(a, b, c)	$(a, b), (a * c, b * c)$	$(a, c), (c, c)$	$(b, c), (b, c)$	1
(6)	(a, b, c)	$(a, b), (a * c, b * c)$	$(a, c), (a * b, c)$	$(b, c), (b, c)$	0

TABLE 1. Types of triple points colored by R_5.

Note that we can apply this classification on other dihedral quandles whose orders are odd and at least five.

3.3. **Admissible 4-tuple of types.** We consider combinations of types of colors of four triple points, and divide them into nine cases below. Let D be a diagram with four triple points, τ_1, τ_2, τ_3 and τ_4. Assume D is colored by R_5. There are six types of colors of a triple point by the previous subsection. Moreover, the total number of triple points of type (4) or (5) is four, two, or zero by Lemma 4.2 which will be given in the next section. The rest of the four triple points are degenerate, i.e., triple points of type (1), (2) or (3), or of type (6). The cases given by changing some of the subscripts of τ_i ($i = 1, 2, 3$, and 4) in a case will be regarded as the same case. These nine cases cover all possible combinations of types of four triple points.

Case I. When all triple points of D are of type (4) or (5).
Case II. When τ_1 and τ_2 are of type (4) or (5), and τ_3 and τ_4 are degenerate.
Case III. When τ_1 and τ_2 are of type (4) or (5), τ_3 is degenerate, and τ_4 is of type (6).
Case IV. When τ_1 and τ_2 are of type (4) or (5), and τ_3 and τ_4 are of type (6).
Case V. When all triple points of D are degenerate.
Case VI. When the type of the color of τ_1 is (6), and τ_2, τ_3 and τ_4 are degenerate.
Case VII. When τ_1 and τ_2 are of type (6), and τ_3 and τ_4 are degenerate.
Case VIII. When τ_1, τ_2 and τ_3 are of type (6), and τ_4 is degenerate.
Case IX. When all triple points are of type (6).

A pair of two triple points, say $\{\tau, \tau'\}$, is called a *canceling pair* if τ and τ' have the same color and opposite signs.

Proposition 3.1. *For any diagram D with four triple points colored by R_5, the triple points satisfy either of the following conditions:*

(i) They form two canceling pairs.
(ii) They form a canceling pair and two degenerate triple points.
(iii) They form four degenerate triple points.

Proof. For each case above, let us verify the proposition.
Case I. There are five cases of types of colors of four triple points which are shown in the table below.

	τ_1	τ_2	τ_3	τ_4
I_1	(4)	(4)	(4)	(4)
I_2	(4)	(4)	(4)	(5)
I_3	(4)	(4)	(5)	(5)
I_4	(4)	(5)	(5)	(5)
I_5	(5)	(5)	(5)	(5)

Since Cases I_4 and I_5 are reduced to other cases by reversing the orientation of F, it is sufficient to consider Cases I_1, I_2, and I_3.

Let us consider the colors of edges for each case. There are four triple points, and 24 parts of edges around the triple points. One of the endpoints of a part is a triple point. The triple points are of type (4) or (5) by the above table, and so the color of each triple point is represented by (a, b, a) or (a, b, c) by Table 1, where a, b and c denote different elements of R_5, and $c = a * b$. Make all combinations of colors of four triple points in R_5. Then for each combination, consider making a graph of 24 colored parts, which is the singular set of a diagram. By Lemma 4.1 in the next section, nondegenerate edges join triple points. So the numbers of parts of nondegenerate edges with the same colors must be even. Therefore, if a combination have an odd number of parts of nondegenerate edges with the same color, it will be ruled out.

We find that there are no possible combinations in Case I_2 by using computer. Computer may be used only for counting the numbers of parts with the same colors. It will not take so much time to be given the result by computer.

Among combinations in Cases I_1 and I_3 which survived in the above process, ten combinations in Case I_3 satisfy the condition in Table 2. In this table, $c = a*(b*a)$. Consider connections of parts of edges in this table. The b/m-edges of τ_1 and τ_2 with the same colors must be connected as depicted in Figure 5 (2). So they are ruled out by Lemma 4.4.

τ	color of τ	edges at τ		
		b/m-edges	b/t-edges	m/t-edges
τ_1	(a, b, a)	$(a, b), (a, b * a)$	$(a, a), (a * b, a)$	$(b, a), (b, a)$
τ_2	$(a, b * a, a)$	$(a, b * a), (a, b)$	$(a, a), (c, a)$	$(b * a, a), (b * a, a)$
τ_3	$(a * b, b, a)$	$(a * b, b), (c, b * a)$	$(a, b), (a * b, b)$	$(b, a), (b, a)$
τ_4	$(c, b * a, a)$	$(c, a), (a * b, b)$	$(c, a), (a, a)$	$(b * a, a), (b * a, a)$

TABLE 2. Ten combinations of colors in Case I_3

For the rest of survived combinations in Cases I_1 and I_3, we can verify that each of them satisfies the condition (i) by using computer in checking.

Case II. It is sufficient to consider the cases below by reversing the orientation of F.

	τ_1	τ_2	τ_3	τ_4
II_1	(4)	(4)	(1)	(1)
II_2	(4)	(5)	(1)	(1)
II_3	(4)	(4)	(1)	(2)
II_4	(4)	(5)	(1)	(2)
II_5	(4)	(4)	(1)	(3)
II_6	(4)	(5)	(1)	(3)
II_7	(4)	(4)	(2)	(2)
II_8	(4)	(5)	(2)	(2)
II_9	(4)	(4)	(2)	(3)
II_{10}	(4)	(5)	(2)	(3)
II_{11}	(4)	(4)	(3)	(3)
II_{12}	(4)	(5)	(3)	(3)

After checking combinations which have odd numbers of parts of nondegenerate edges with the same colors, we find that all combinations in Case II_2, II_4, II_6, II_8, II_{10}, and II_{12} are ruled out. Then we can verify that each survived combination in Case II satisfies the condition (ii).

Case III. It is sufficient to consider the cases below by reversing the orientation of F.

	τ_1	τ_2	τ_3	τ_4
III_1	(4)	(4)	(1)	(6)
III_2	(4)	(5)	(1)	(6)
III_3	(4)	(4)	(2)	(6)
III_4	(4)	(5)	(2)	(6)
III_5	(4)	(4)	(3)	(6)
III_6	(4)	(5)	(3)	(6)

After checking combinations which have odd numbers of parts of nondegenerate edges with the same colors, we find that all combinations in Cases III_2, III_4, and III_6 are ruled out.

For each survived combination, if it has a connection as depicted in Figure 5 (1), then it will be ruled out by Lemma 4.4. After doing this process, we find that there are no possible combinations in Cases III_1, III_3, and III_5.

Case IV. It is sufficient to consider the cases below by reversing the orientation of F.

	τ_1	τ_2	τ_3	τ_4
IV_1	(4)	(4)	(6)	(6)
IV_2	(4)	(5)	(6)	(6)

After checking combinations which have odd numbers of parts of nondegenerate edges with the same colors, and which have connections as depicted in Figure 5 (1), we find that all combinations in Case IV_2 are ruled out. Then we can verify that each survived combination in Case IV_1 satisfies the condition (i).

Case V. All combinations satisfy the condition (iii) by the definition of Case V.

Case VI. It is sufficient to consider the cases below by reversing the orientation of F.

	τ_1	τ_2	τ_3	τ_4
VI_1	(6)	(1)	(1)	(1)
VI_2	(6)	(1)	(1)	(2)
VI_3	(6)	(1)	(1)	(3)
VI_4	(6)	(1)	(2)	(2)
VI_5	(6)	(1)	(2)	(3)
VI_6	(6)	(1)	(3)	(3)
VI_7	(6)	(2)	(2)	(2)
VI_8	(6)	(2)	(2)	(3)
VI_9	(6)	(2)	(3)	(3)
VI_{10}	(6)	(3)	(3)	(3)

After checking combinations which have odd numbers of parts of nondegenerate edges with the same colors, we find that all combinations in Case VI are ruled out.
Case VII. It is sufficient to consider the cases below by reversing the orientation of F.

	τ_1	τ_2	τ_3	τ_4
VII_1	(6)	(6)	(1)	(1)
VII_2	(6)	(6)	(1)	(2)
VII_3	(6)	(6)	(1)	(3)
VII_4	(6)	(6)	(2)	(2)
VII_5	(6)	(6)	(2)	(3)
VII_6	(6)	(6)	(3)	(3)

After checking combinations which have odd numbers of parts of nondegenerate edges with the same colors, we can verify that each survived combination satisfies the condition (ii).
Case VIII. It is sufficient to consider the cases below by reversing the orientation of F.

	τ_1	τ_2	τ_3	τ_4
VIII_1	(6)	(6)	(6)	(1)
VIII_2	(6)	(6)	(6)	(2)
VIII_3	(6)	(6)	(6)	(3)

After checking combinations which have odd numbers of parts of nondegenerate edges with the same colors, we find that all combinations in Case VIII are ruled out.
Case IX. After checking combinations which have odd numbers of parts of nondegenerate edges with the same colors, and which have connections as depicted in Figure 5 (1), 30 combinations among survived combinations satisfy either of the following conditions (A), (B), and (C).

(A) There are ten combinations shown in Table 3, and in the table, $a * c = b$. We can see that the b/m-edges of τ_1 and τ_3 must be connected as depicted in Figure 5 (2). So they are ruled out by Lemma 4.4.

(B)There are ten combinations shown in Table 4, and in the table, $a * c = b$. We can see that the b/m-edges of τ_1 and τ_2 must be connected as depicted in Figure 5 (2). So they are ruled out by Lemma 4.4.

τ	color of τ	edges at τ		
		b/m-edges	b/t-edges	m/t-edges
τ_1	(a, b, c)	$(a, b), (b, a)$	$(a, c), (a * b, c)$	$(b, c), (b, c)$
τ_2	$(a, a * b, c)$	$(a, a * b), (b, b * a)$	$(a, c), (b * a, c)$	$(a * b, c), (a * b, c)$
τ_3	(b, a, c)	$(b, a), (a, b)$	$(b, c), (b * a, c)$	$(a, c), (a, c)$
τ_4	$(b, b * a, c)$	$(b, b * a), (a, a * b)$	$(b, c), (a * b, c)$	$(b * a, c), (b * a, c)$

TABLE 3. Ten combinations of colors in Case IX (A)

τ	color of τ	edges at τ		
		b/m-edges	b/t-edges	m/t-edges
τ_1	(a, b, c)	$(a, b), (b, a)$	$(a, c), (a * b, c)$	$(b, c), (b, c)$
τ_2	(b, a, c)	$(b, a), (a, b)$	$(b, c), (b * a, c)$	$(a, c), (a, c)$
τ_3	$(a * b, b, c)$	$(a * b, b), (b * a, a)$	$(a * b, c), (a, c)$	$(b, c), (b, c)$
τ_4	$(b * a, a, c)$	$(b * a, a), (a * b, b)$	$(b * a, c), (b, c)$	$(a, c), (a, c)$

TABLE 4. Ten combinations of colors in Case IX (B)

(C)There are ten combinations shown in Table 5, and in the table, $a * c = b, d = a * b$, and $e = b * a$. We can see that the b/m-edges of τ_1 and τ_2 must be connected as depicted in Figure 5 (2). So they are ruled out by Lemma 4.4.

τ	color of τ	edges at τ		
		b/m-edges	b/t-edges	m/t-edges
τ_1	(a, b, c)	$(a, b), (b, a)$	$(a, c), (d, c)$	$(b, c), (b, c)$
τ_2	(b, a, c)	$(b, a), (a, b)$	$(b, c), (e, c)$	$(a, c), (a, c)$
τ_3	(d, e, c)	$(d, e), (e, d)$	$(d, c), (b, c)$	$(e, c), (e, c)$
τ_4	(e, d, c)	$(e, d), (d, e)$	$(e, c), (a, c)$	$(d, c), (d, c)$

TABLE 5. Ten combinations of colors in Case IX (C)

Then for each of the rest of survived combinations in Case IX, we can verify that it satisfies the condition (i). □

3.4. **Admissible 5-tuple of types.** When a diagram has five triple points, we can obtain a similar proposition.

Proposition 3.2. *For any diagram with five triple points colored by R_5, the triple points satisfy either of the following conditions:*

(i) They form two canceling pairs and a degenerate triple point.
(ii) They form a canceling pair and three degenerate triple points.
(iii) They form five degenerate triple points.

Proof. Taking the same process in the previous subsection in the case of four triple points, we can reach the result that the triple points satisfy either of (i), (ii), and (iii).

We can use Lemma 4.3 as a step to return to the case of four triple points. □

3.5. **Proof of Theorem 1.1.**

Proof. We show that if $t(F) \leq 5$, then $\Phi_\theta(F) \in \mathbb{Z}$ for any 3-cocycle $\theta : R_5 \times R_5 \times R_5 \to G$. It is sufficient to show that if $t(F) \leq 5$, then $W_\theta(C) = 1_G$ for any color C in R_5 by the definition of $\Phi_\theta(F)$. Satoh and Shima showed the case when $t(F) \leq 3$ in [11]. So it is sufficient to consider the case when a surface-knot diagram D has four or five triple points.

When D has four triple points, τ_1, τ_2, τ_3 and τ_4, and a color C in R_5, the triple points satisfy (i), (ii), or (iii) in Proposition 3.1. If they satisfy (i), then

$$W_\theta(\tau_1; C) \cdot W_\theta(\tau_2; C) = 1_G, \quad W_\theta(\tau_3; C) \cdot W_\theta(\tau_4; C) = 1_G.$$

Hence,

$$\begin{aligned} W_\theta(C) &= W_\theta(\tau_1; C) \cdot W_\theta(\tau_2; C) \cdot W_\theta(\tau_3; C) \cdot W_\theta(\tau_4; C) \\ &= 1_G \cdot 1_G \\ &= 1_G. \end{aligned}$$

If they satisfy (ii), then

$$W_\theta(\tau_1; C) \cdot W_\theta(\tau_2; C) = 1_G, \quad W_\theta(\tau_3; C) = W_\theta(\tau_4; C) = 1_G.$$

Hence,

$$W_\theta(C) = 1_G \cdot 1_G \cdot 1_G = 1_G.$$

If they satisfy (iii), then

$$W_\theta(\tau_1; C) = W_\theta(\tau_2; C) = W_\theta(\tau_3; C) = W_\theta(\tau_4; C) = 1_G.$$

Hence,

$$W_\theta(C) = 1_G \cdot 1_G \cdot 1_G \cdot 1_G = 1_G.$$

When D has five triple points, τ_1, τ_2, τ_3, τ_4 and τ_5, and a color C in R_5, the triple points satisfy (i), (ii), or (iii) in Proposition 3.2. If they satisfy (i), then

$$W_\theta(\tau_1; C) \cdot W_\theta(\tau_2; C) = 1_G, \quad W_\theta(\tau_3; C) \cdot W_\theta(\tau_4; C) = 1_G, \quad W_\theta(\tau_5; C) = 1_G.$$

Hence,

$$W_\theta(C) = 1_G \cdot 1_G \cdot 1_G = 1_G.$$

If they satisfy (ii), then

$$W_\theta(\tau_1; C) \cdot W_\theta(\tau_2; C) = 1_G, \quad W_\theta(\tau_3; C) = W_\theta(\tau_4; C) = W_\theta(\tau_5; C) = 1_G.$$

Hence,

$$W_\theta(C) = 1_G \cdot 1_G \cdot 1_G \cdot 1_G = 1_G.$$

If they satisfy (iii), then

$$W_\theta(\tau_1; C) = W_\theta(\tau_2; C) = W_\theta(\tau_3; C) = W_\theta(\tau_4; C) = W_\theta(\tau_5; C) = 1_G.$$

Hence,

$$W_\theta(C) = 1_G \cdot 1_G \cdot 1_G \cdot 1_G \cdot 1_G = 1_G.$$

After all, we see that

$$W_\theta(C) = 1_G$$

for each admissible color C in R_5. This completes the proof. □

4. Complements to the proof of theorem 1.1

In Section 4.1 we show some lemmas, which were used in the proof of Theorem 1.1 in Section 3. In Section 4.2 we review Alexander numberings for surface-knots, which is useful when we find which combinations of colored triple points are ruled out.

4.1. **Some lemmas for Section 3.** Satoh and Shima showed the following lemmas.

Lemma 4.1 ([10])**.** *Let e be an edge of a surface-knot diagram colored by R_5. If one of the endpoint of e is a branch point, then e is degenerate.*

In [10, Proposition 4.1], Satoh and Shima showed that for any diagram colored by R_3, the number of nondegenerate triple points is always even. Lemma 4.2 is another way to state this proposition.

Lemma 4.2. *Let n be an odd and at least five, and R_n the dihedral quandle of order n. For any surface-knot diagram colored by R_n, the total number of triple points of type (4) or (5) is always even.*

Proof. Let B and E_0 be the numbers of branch points and degenerate edges of a surface-knot diagram colored by R_n respectively, and let $\{\tau_1, ..., \tau_s\}$ be the set of triple points of the diagram. By counting degenerate edges around branch points and triple points, we have the identity

$$2E_0 = B + \sum_{i=1}^{s} d(\tau_i)$$

by Lemma 4.1. Since the number of branch points in each connected component of a singular set is always even, B is even. So we see that $\sum_{i=1}^{s} d(\tau_i)$ is even in the above equation. On the other hand, since $d(\tau) = 0, 1, 2$, or 6 by Table 1, $\sum_{i=1}^{s} d(\tau_i)$ has the same parity as the number of triple points with $d(\tau_i) = 1$. $d(\tau_i) = 1$ if and only if τ_i is of type (4) or (5). And so we have the conclusion. □

Lemma 4.3 is used in the proof of Proposition 3.2 in Section 3.4. Roseman moves [1] are moves among diagrams, which relate diagrams representing isotopic surface-knots.

Lemma 4.3 ([10])**.** *Let e be an edge of a surface-knot diagram whose endpoints are a branch point and a triple point τ. If e is a b/m- or m/t-edge at τ, then we can remove τ by some Roseman moves in a neighborhood of e.*

4.2. **Alexander numberings.** Let F be an oriented surface-knot, and $\pi : \mathbb{R}^4 \to \mathbb{R}^3$ a generic projection for F. To each region of $\mathbb{R}^3 \setminus \pi(F)$ we assign an integer with the following rules:

(a) The integer of the unbounded region is 0,
(b) Regions that are separated by a sheet are numbered consecutively.
(c) The normal vector to $\pi(F)$ points towards the region with larger integer.

See Figure 4. Such an indexing is called an *Alexander numbering*. The number of a region assigned by the Alexander numbering represents the number of walls separating the region from the unbounded region, counted with sign.

We can also define the Alexander numbering by another way. Let us take a point a in the region which we want to know the number assigned by the Alexander numbering. Then take a sphere whose center is a, and consider a map $g : F \to S^2$

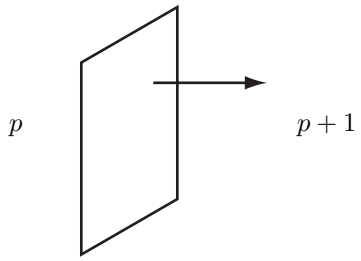

FIGURE 4. The Alexander numbering

given by $x \mapsto \frac{\pi(x)-a}{\|\pi(x)-a\|}$. The mapping degree of this map is the assigned number of the region. Therefore, the first definition of the Alexander numbering is well defined.

Lemma 4.4. *For any diagram of a surface-knot, it is impossible to connect edges as depicted in Figure 5 (1) and (2) respectively.*

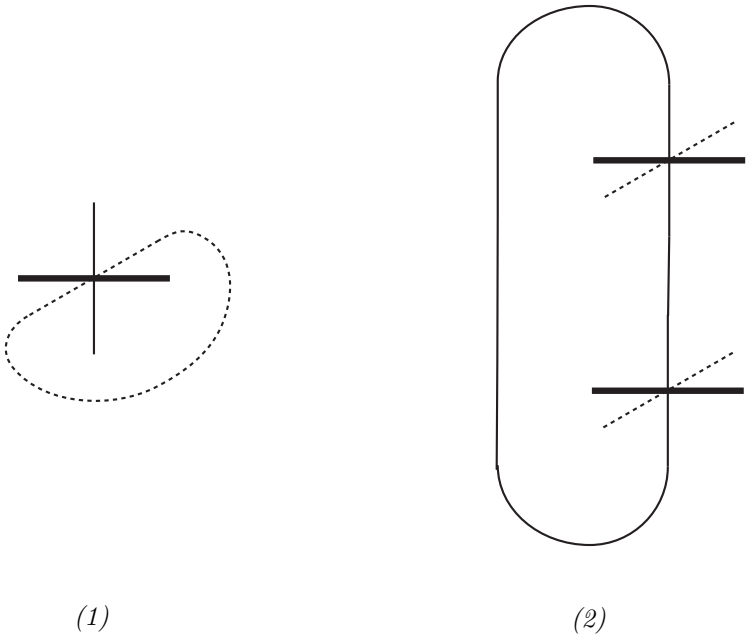

FIGURE 5. Impossible connections of edges. Thin lines, thick lines and dotted lines denote the same in Figure 3.

Proof. (1) Consider what happens in a neighborhood of the graph in Figure 5 (1). See Figure 6. Assume that one of the regions to which normal vectors to the top and the middle sheet point has the Alexander numbering p. If the normal vector to the bottom sheet points as depicted in Figure 6, then this region has also the Alexander numbering $p+1$. If the normal vector to the bottom sheet points reversely, then this region has the Alexander numbering $p-1$. This is a contradiction in either case.

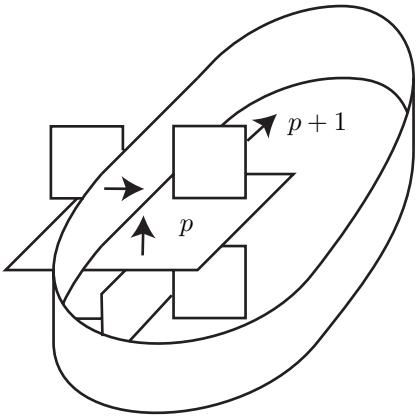

FIGURE 6. A diagram in a neighborhood of the graph in Figure 5 (1).

(2) Let τ_1 and τ_2 denote the two triple points in Figure 5 (2). Let us consider the diagram in a neighborhood of the graph. See Figure 7. There are two regions, $\mathcal{R}_1$ and $\mathcal{R}_2$. Assume that $\mathcal{R}_1$ has the Alexander numbering p. Then $\mathcal{R}_2$ has the number $p+1$ by the direction of the normal vector to the top sheet of τ_1. Moreover, $\mathcal{R}_1$ has also the number $p+2$ by the direction of the normal vector to the top sheet of τ_2. This is a contradiction.

□

5. Examples

In this section, we give two examples which we can obtain better estimates of the triple point numbers using Theorem 1.1. Let $\theta : R_5 \times R_5 \times R_5 \to \mathbb{Z}_5 = \langle u | u^5 = 1 \rangle$ be the 3-cocycle given in (♯). We use Theorem 5.1 to obtain an upper bound of the triple point number of a surface-knot.

Theorem 5.1 ([10])**.** *If a classical knot K has a knot diagram with c crossings in which there is a pair of crossings as shown in Figure 8, then we have $t(\tau^m K) \leq 2(c-2)m$, where $\tau^m K$ denotes the m-twist-spun of K.*

5.1. **The 2-twist-spun figure eight knot.** We denote the 2-twist-spun figure eight knot by F in this subsection. F has a diagram which has 8 triple points by Theorem 5.1. For the diagram, we have the identity

$$\Phi_\theta(F) = 5 + 10u + 10u^4 \notin \mathbb{Z} \subset \mathbb{Z}[\mathbb{Z}_5],$$

by using computer for calculations. Refer to [10] for the structure of diagrams and colors of twist spun of knots. Hence we see that $6 \leq t(F) \leq 8$ by Theorem 1.1.

5.2. **The 2-twist-spun $(2,5)$-torus knot.** We denote the 2-twist-spun $(2,5)$-torus knot by $\tau^2 T_{2,5}$. By using computer for calculations, we have the identity

$$\Phi_\theta(\tau^2 T_{2,5}) = 5 + 10u^2 + 10u^3 \notin \mathbb{Z} \subset \mathbb{Z}[\mathbb{Z}_5].$$

Refer to [7] for diagrams and colors of twist spun of $(2,n)$-torus knots. On the other hand, $\tau^2 T_{2,5}$ has a diagram which has 12 triple points by Theorem 5.1. So we see that $6 \leq t(\tau^2 T_{2,5}) \leq 12$ by Theorem 1.1.

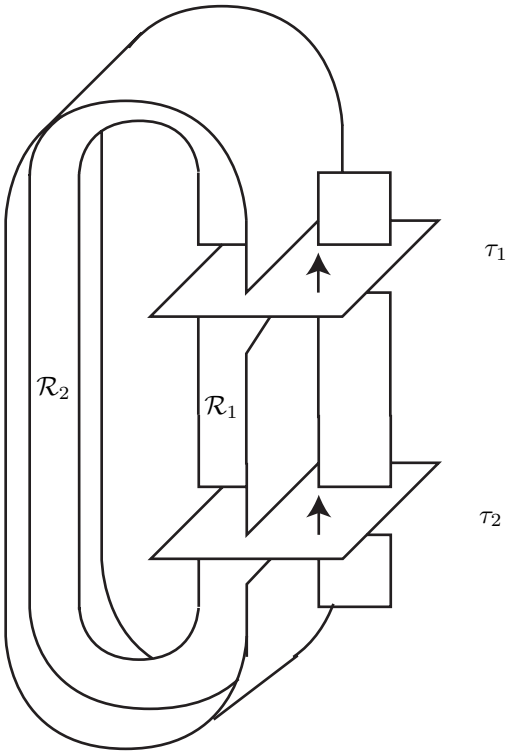

FIGURE 7. A diagram in a neighborhood of the graph in Figure 5 (2).

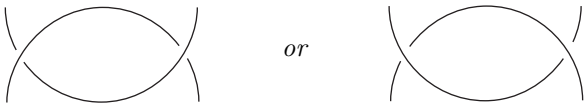

FIGURE 8

REFERENCES

[1] J. S.Carter, M.Saito, *Knotted Surfaces and their diagrams*, Surveys and monographs the American Mathematical Society, 1998.

[2] J. S. Carter, D. Jelsovsky, S.Kamada, L.Langford and M. Saito, *Quandle cohomology and state-sum invariants of knotted curves and surfaces*, preprint (math.GT/9903135).

[3] J. S. Carter, S. Kamada, and M. Saito, *Alexander Numbering of Knotted Surface Diagram*, Proc. Amer. Math. Soc. **128** no 12 (2000) 3761–3771.

[4] T. Mochizuki, *Some calculations of cohomology groups of finite Alexander quandles*, (2002) preprint at http://www.math.ias.edu/ takuro/.

[5] T. Mochizuki, *The 3-cocycles of the Alexander quandles* $\mathbb{F}_q[T]/(T-\omega)$, preprint (math.GT/0210419).

[6] S.Satoh, *On non-orientable surfaces in 4-space which are projected with at most one triple point*, Proc. Amer. Math. Soc. **128** (2000), no. 9, 2789–2793.

[7] S. Satoh, *On cocycle invariants of twist-spun (2,n)-torus knots*, preprint.

[8] S. Satoh, *Triple point numbers of non-ribbon 2-knots are grater than three*, (2002), preprint.

[9] A. Shima, *Knotted 2-spheres whose projections into 3-space contain at most two triple points are ribbon 2-knots*, preprint.

[10] S. Satoh and A. Shima, *The 2-twist-spun trefoil has the triple point number four*, preprint.

[11] S. Satoh and A. Shima, in prepararion.
[12] T. Yajima, *on simply knotted spheres in* R^4, Osaka J. Math. **1** (1964), 133–152.

Department of Mathematics, Tokyo Institute of Technology, 2-12-1, O-okayama, Meguro-ku, Tokyo, 152-8550, Japan
E-mail address: hataken0@is.titech.ac.jp